

Disulfide-Intact and -Reduced Lysozyme in the Gas Phase: Conformations and Pathways of Folding and Unfolding

Stephen J. Valentine, Jennifer G. Anderson, Andrew D. Ellington, and David E. Clemmer*

Department of Chemistry, Indiana University, Bloomington, Indiana 47405

Received: January 14, 1997; In Final Form: March 5, 1997[⊗]

The conformations of gaseous lysozyme ions (+5 through +18) produced by electrospray ionization have been studied in the gas phase using ion mobility mass spectrometry techniques. When solutions containing the disulfide-intact and disulfide-reduced lysozyme are electrosprayed, the gas-phase ions that are produced have distinctly different collision cross sections. Disulfide-intact ions favor two conformer types: a highly folded conformer with a cross section near that calculated for the crystal structure and a partially unfolded conformer that is formed when the ions are injected into the drift tube at high injection voltages. Ions formed from the disulfide-reduced solution have collision cross sections that are much larger than any observed for the disulfide-intact protein, showing that these ions are largely unfolded. Gas-phase proton-transfer reactions in the ion source can be used to favor lower charge states for both solutions. When protons are removed from disulfide-intact lysozyme ions, highly folded compact conformations are favored. Exposing the disulfide-reduced lysozyme ions to proton-transfer reagents causes the protein to fold up, and several of the new conformations have cross sections that are indistinguishable from those measured for the disulfide-intact protein. It appears that an array of gas-phase folding intermediates or misfolded metastable states are stable because of the well-defined interplay between attractive–folding and repulsive–Coulombic interactions.

Introduction

Characterizing the shapes and sizes of large biomolecules presents significant challenges for chemists due to the overwhelming sizes of these molecules. Techniques such as NMR and crystallography have proven to be powerful structural probes of low-lying native or crystal states (in some cases providing atomic details). For the most part there is only vague understanding of the structures of partially organized non-native proteins, mainly because of the transient nature of these species. New ionization sources such as electrospray ionization (ESI)¹ and matrix-assisted laser desorption ionization (MALDI)² have made it possible to create large biomolecular ions for analysis with mass spectrometry (MS) techniques. Measurements of accurate molecular weights are becoming routine,^{3,4} and many new MS-based strategies for sequencing biopolymers are being examined and developed.^{5–10} An issue that has emerged is the structure of the gas-phase ion. If the gas-phase protein ion retains some degree of “memory” of its solution conformation, then techniques such as mass spectrometry, which are inherently fast and sensitive, may be useful for characterizing conformations of biomolecules. If protein conformations in the gas phase are vastly different than in solution, then structural information will help guide our understanding of the influence of solvents on structure. A fundamental understanding of roles of intra-protein forces and solvent–protein interactions is central to many unresolved biochemical issues, including protein folding.

In this paper we have examined the conformations of disulfide-intact and disulfide-reduced lysozyme ions in the gas phase using ion-mobility techniques.^{11–14} Lysozyme is made up of 129 amino acids and in its native state has four covalent disulfide linkages between the 6–127, 30–115, 64–80, and 76–94 cystine residues. When the disulfide bonds are reduced in solution, the protein denatures, and when the reducing conditions are removed, the protein refolds.^{15–18} It has been proposed that reformation and misformation of disulfide bonds

could be critical steps in the renaturation of reduced lysozyme, leading to multiple intermediates and pathways for folding.^{15,17} The effect of disulfide bonds upon the fragmentation patterns of multiply charged protein ions is pronounced, presumably because the ESI parent ions have different conformations.¹⁹

Recent evidence suggests that it is possible to induce structural changes in gas-phase proteins ions by subjecting them to high-energy collisions, UV radiation, and proton-transfer reactions.^{20–22} Williams and co-workers have used Fourier transform ion cyclotron resonance (FTICR) techniques to measure the proton-transfer rate constants for reactions of disulfide-intact and disulfide-reduced lysozyme ions with different bases and have bracketed values for the gas-phase basicities of the different charge states.²¹ By comparing their measured apparent basicities to values that they calculated for the crystal structure and a one-dimensional string model conformation of lysozyme, they inferred structural information about the ions. Although this method for deducing structures is indirect and has not been tested, the comparison is striking. Disulfide-intact and -reduced ions, formed by ESI source, display conformers with apparent gas-phase basicities that fall along the values calculated for the crystal and one-dimensional string models, respectively. After ions were exposed to proton-transfer reagents, the measured basicities for the disulfide-intact ions are larger than those predicted for the crystal conformer, suggesting that the disulfide-intact conformer unfolds as protons are removed. After protons were removed from the disulfide-reduced ions, the measured basicities fall below the model for the one-dimensional string, suggesting that the disulfide-reduced protein folds as charges are removed.

The ion-mobility measurements presented here provide direct information about the conformations of the lysozyme ions. The mobility of a gas-phase ion depends on its collision cross section with a buffer gas, which is defined by its geometry. Conformations having different collision cross sections can be separated based on variations in their mobilities.²³ By comparing experimentally measured mobilities (or cross sections) to those

[⊗] Abstract published in *Advance ACS Abstracts*, April 15, 1997.

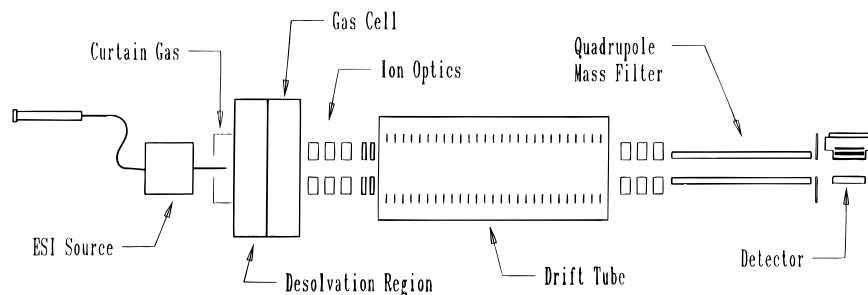


Figure 1. Schematic diagram of the experimental apparatus.

that are calculated for trial geometries, it is possible to obtain direct structural information about the ion. This method has been used to deduce the gas-phase structures of a number of atomic cluster²⁴ and complex ion systems^{25,26} and has recently been extended to study protein conformations in the gas phase.^{23,25,27,28} A powerful feature of this technique is that by varying the energy that is used to inject the ions into the high-pressure drift tube, it is possible to induce and follow changes in structure.^{29,30} As the ions enter the drift tube, their kinetic energy is thermalized by collisions with the buffer gas, causing a rapid transient heating cycle that can induce structural changes. The resulting ion-mobility spectra record whether more compact or diffuse structures are formed. We take advantage of this method of inducing structural changes to probe transitions in the disulfide-intact and -reduced lysozyme. The data presented here are the first measurements of the collision cross sections of disulfide-intact and -reduced lysozyme.

In addition to ion-mobility measurements of cross sections^{23,25,27,28} and FTICR measurements of gas-phase basicities,^{21,31} several other techniques are emerging to provide structural information about gas-phase biomolecules. Isotopic H/D exchange, which is based on differences in the number of accessible heteroatom hydrogens, is being developed to investigate the conformations of oligopeptides³² and proteins.^{20,33–35} McLafferty and co-workers have shown that multiple conformations can be resolved and structural transitions resulting from proton-transfer reactions can be studied.²⁰ We have recently carried out H/D exchange of shape-resolved conformers of cytochrome *c* in a drift tube and shown that it is possible to simultaneously characterize the number of exchangeable hydrogens and overall shape of the ions.²⁸ Douglas,^{36–38} Cooks,³⁹ and their co-workers have used triple quadrupole instruments to measure the ion energy losses of protein ions passing through buffer gasses. These results were the first to show that protein ions in different charge states have different collision cross sections, a result that was also derived from ion-mobility studies,²³ and microscopy studies of the surface imprints that are found after high-energy protein collisions.⁴⁰ Macromolecular ions in low charge states have been analyzed using differential mobility techniques, and electrical mobility diameters have been reported.⁴¹ A number of other ion-mobility^{42–44} and ion molecule reaction studies^{33,45–47} for biological ions have been carried out, although no detailed structural information was derived from these data.

Experimental Section

General. Ion-mobility techniques have been described in detail previously.^{11–14} Here, we describe our instrument and the typical conditions used for these studies. A schematic diagram of the experimental apparatus is shown in Figure 1. Multiply charged lysozyme ions are formed in an ESI source that is similar to one described by Smith and co-workers.⁴⁸ The electro-spray needle and entrance region are enclosed in a

plexiglass case that allows a curtain of dry nitrogen gas to purge the entrance region. Electro-sprayed droplets are formed at atmospheric pressures and enter a variable-temperature, differentially pumped desolvation region through a 0.1 cm diameter entrance orifice. Ions pass through this region and exit through another 0.1 cm aperture, where they enter the source gas cell. The diameters of the entrance and exit apertures for the desolvation region and gas cell can be varied easily. The pressure in each of these regions is ~ 1 –10 Torr, depending on apertures that are used. The length of the desolvation and gas-cell regions can also be varied (from ~ 4 to ~ 14 cm). Most of the studies reported below were carried out using desolvation region and gas-cell lengths of 4.4 cm each. For both the disulfide-intact and -reduced systems (where no proton-transfer reagents were used), a smaller number of studies was carried out where the gas-cell region was removed. The resulting drift time distributions and mass spectra were indistinguishable from those obtained with the desolvation region/gas-cell configuration shown in Figure 1 before the proton-transfer reagent was added. This confirms that the ions we are examining are desolvated before leaving the desolvation region.

For proton-transfer studies, a small amount of a base [either *n*-butylamine or 7-methyl-1,5,7-triazabicyclo[4.4.0]dec-5-ene (MTBD) with gas-phase basicities of 210.6 kcal/mol⁴⁹ and 243.3 kcal/mol,⁵⁰ respectively] was introduced into the gas-cell region. Base was added by monitoring the ion signal while introducing base vapor through a leak valve. The presence of the base causes dramatic variations in the ion signals for different charge states, and at the first sign of a change in signal, the setting on the leak valve was decreased slightly and we began collecting data. Under these conditions, the partial pressure of base could not be discerned from the background pressure of the gas cell. Mass spectra, acquired before and after base was added to the gas cell, confirm that proton-transfer reactions have occurred as discussed below.

Lysozyme ions exit the source region through another 0.08 cm diameter aperture and enter a high-vacuum region (10^{-4} – 10^{-5} Torr) where they are focused into a low-energy ion beam and injected into the drift tube containing ~ 2 Torr of helium buffer gas. The buffer gas pressure inside the drift tube is measured using a capacitance manometer. The drift tube is 32.4 cm long with 0.08 cm diameter entrance and exit apertures and comprises 26 equally spaced electrostatic lenses to ensure a uniform electric field. The drift tube body is made of stainless steel with Teflon spacers at each end, which electrically isolate the entrance and exit plates. In these studies, a nominal drift field (E) of 14.0 V cm^{-1} was applied across the drift tube. We define an effective drift field as zE , a value that depends on the charge state (and also leads to an effective increase in the ability to resolve peaks with increasing charge state). We carried out a series of diagnostic studies of the drift velocity as a function of the drift field to ensure that all charge states remained in the low-field limit.⁵¹ After exiting the drift tube, ions are focused

into a quadrupole mass spectrometer that can be set to transmit a specific mass (for measurements of drift time distributions) or scanned in order to monitor product formation (in the case of proton-transfer reaction studies).

Electrospraying Disulfide-Intact and Disulfide-Reduced Lysozyme Solutions. The ESI charge state distributions for lysozyme depend on the properties of the solution.^{21,52} In these experiments the disulfide-intact solution was 7.0×10^{-5} M in lysozyme (turkey, Sigma >99%) in a 1:1 water:acetonitrile mixture which also contained 0.2% acetic acid. The disulfide-reduced form of lysozyme was obtained by boiling a lysozyme:water:0.02 M dithiothreitol solution for 30 min as described previously.²¹ The resulting solution was diluted with hot (~ 60 °C) acetonitrile and acetic acid such that the electrosprayed solution was $\sim 1:1$ water:acetonitrile with 0.2% acetic acid. The electrospray syringe, tubing, and needle were all maintained at 60 °C to ensure that all of the disulfide bonds remained reduced. With an analogous procedure, high-resolution FTICR mass spectra show an 8 amu increase in mass for reduced lysozyme compared with the native protein, demonstrating that all four of the disulfide bonds were reduced.²¹

Conformer Separation. Different protein conformations within a given charge state are separated because of differences in their mobilities.²³ Ion mobility spectra were recorded by injecting 0.030–0.050 ms ion pulses into the drift tube and recording the arrival time distribution at the detector with a multichannel scaler. The arrival time is a composite of the drift time in the drift tube and time required for the ion pulse to travel through other portions of the instrument before reaching the detector. Thus, it is necessary to subtract the flight time of the ions when no buffer gas is present and also account for the fact that the ions' energies at the exit of the drift tube, with and without buffer gas, are different. Under the conditions of our current experiments, differences between the arrival time and drift times were usually between 0.25 and 0.35 ms.

Compact conformers have larger mobilities (and smaller collision cross section) than more diffuse ones. The reduced mobility is determined from⁵¹

$$K_0 = \frac{L}{t_D E} \frac{P}{760} \frac{273.2}{T} \quad (1)$$

where t_D is the average drift time, E is the electric field, L is the length of the drift tube, and P is the pressure in Torr. As in electrophoresis, the mobility also depends upon the charge state of the ion, with higher charge states having higher mobilities. Thus, for characterizing conformations, it is simplifying to convert the data into collision cross sections, which account for the charge state. These are derived directly from the experimental data using the expression

$$\Omega = \frac{(18\pi)^{1/2}}{16} \frac{ze}{(k_B T)^{1/2}} \left[\frac{1}{m_I} + \frac{1}{m_B} \right]^{1/2} \frac{t_D E}{L} \frac{760}{P} \frac{T}{273.2} \frac{1}{N} \quad (2)$$

which contains the reduced mobility expression and where z is the charge state, N is the neutral number density, and m_I and m_B are the masses of the ion and buffer gas, respectively. This equation can be rearranged to solve for the drift time under a specific set of experimental conditions, useful for predicting where assumed conformations might appear in the ion-mobility distributions, as discussed below. All of the parameters E , L , P , and t_D can be precisely measured. Thus, the reproducibility of measured mobilities or cross sections in these studies is excellent, with different measurements usually agreeing to within 2%.

Structural Analysis. Information about the shapes of protein conformers present in mobility data can be obtained by comparing the measured collision cross sections to those calculated for trial structures.^{23,27} In this paper, we compare our data to two structures that should provide limits for the collision cross sections that we observe: the crystal structure⁵³ (which should correspond to one of the smallest possible cross sections) and a near-linear conformer,⁵⁴ obtained by straightening the protein out as much as reasonably possible. The collision cross section for a trial set of atomic coordinates averaged over all possible orientations assumes a rigid structure and is estimated from²⁷

$$\Omega_{av}^{(1,1)} \approx \frac{1}{8\pi^2} \int_0^{2\pi} d\theta \int_0^\pi d\phi \sin\phi \int_0^{2\pi} d\gamma \pi b_{min}^2(\theta, \phi, \gamma)^2 \quad (3)$$

where $b_{min}(\theta, \phi, \gamma)$ is the minimum impact parameter for a region defined by the angles θ , ϕ , and γ . This expression is modified with a porosity factor that takes into account the density of the protein, since for diffuse conformers some trajectories may allow He to pass through the protein without undergoing a collision.

Values of b_{min} depend on values of the hard-sphere collision distances which are defined as $b_{hs} = 1/2(d_{atom} + d_{He})$ where d_{He} is 2.2 Å and the diameters of H, C, N, O, and S atoms of the protein are taken to be 2.2, 3.1, 2.8, 2.7, and 3.6 Å, respectively.⁵⁵ For large molecules with dense interiors such as the crystal coordinates of lysozyme, eq 3 is insensitive to the impact parameters used. However, for the near-linear conformer, where many of the atoms are exposed at the surface, the resulting cross section depends strongly on the impact parameters that are used. Since the impact parameters are not rigorously known, we vary them by $\pm 5\%$ in order to provide uncertainties associated with these calculations. With this procedure we estimate cross sections of 1180 ± 30 and 3750 ± 170 Å² for the crystal coordinates and near-linear extended conformation, respectively.

The above treatment of the average cross section ignores more subtle contributions to the cross sections that arise from van der Waals and long-range ion-induced dipole interactions as well as differences in momentum transfer that come about from different trajectories of the colliding partners before and after the collision. For multiply charged ions long-range ion-induced dipole interactions increase with increasing charge state. For cross sections of multiply charged proteins measured in 300 K He, the collision cross section is dominated by the hard-sphere interactions because of the extremely large size of the protein and the very small polarizability of He.²⁷ Augmentations in cross sections (for even the highest charge states) for proteins of this size are less than a few percent, below the uncertainties in the calculated hard-sphere cross sections.

A more important consideration appears to be the scattering trajectories of the buffer gas atoms after the protein–He collision. Shvartsburg and Jarrold have recently shown that hard-sphere calculations of collision cross sections may be influenced as much as $\sim 25\%$ for some conformations by including multiple scattering events in the cross section calculations. Thus, the cross section calculations that we report here are only estimates and are best viewed as lower limits to the true cross sections.

Injection of Ions into the Drift Tube. As ions are injected into the drift tube they undergo a rapid heating cycle as their kinetic energies are thermalized by collisions with the buffer gas. Further collisions cool the ions to the buffer gas temperature. As discussed above, this is a powerful feature of injected ion mobility techniques that allows different conformations to be formed and examined. The ions' kinetic energies are determined by the injection voltage, which we define as the

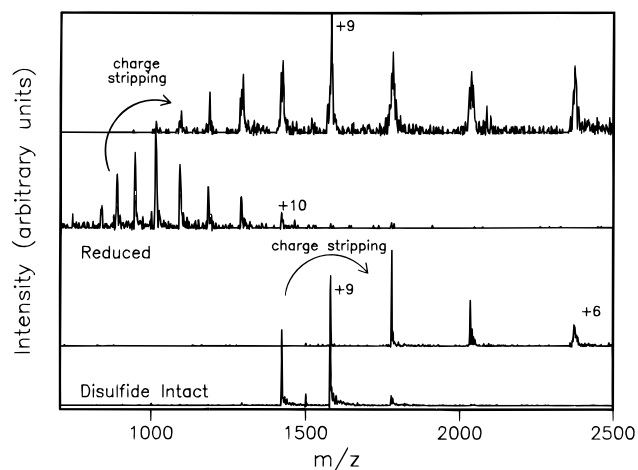


Figure 2. Mass spectra for disulfide-intact and -reduced lysozyme solutions as described in the text. Also shown are the mass spectra obtained when these solutions are exposed to gas-phase charge-stripping reagents in the source.

potential difference between the exit plate of the high-pressure gas cell and the entrance of the drift tube. Injection voltages can be converted into energies by multiplying by the charge state. At high injection voltages a concern that arises is that dissociation or proton-stripping processes may occur. We have studied this by recording ESI mass spectra as a function of injection voltage for cytochrome *c*,²⁸ ubiquitin,⁵⁶ and lysozyme. For all charge states of these proteins, injected into our current drift tube containing ~ 2 Torr of He, mass spectral distributions are independent of the injection voltage used up to ~ 150 – 200 V. In the present studies, there is no evidence that collision-induced dissociation or proton-stripping processes influence our ion-mobility distributions.

In order to examine conformations that are formed in the ion source, it is desirable to use the lowest possible injection voltages. At low injection voltages, studies are limited because of low ion signals. At ~ 30 V signals are about 10 times smaller than those at 120 V. For the disulfide-intact solution, which produces abundant signals, we have carried out extensive studies as a function of the injection voltage, while for the disulfide-reduced solution, where ion signals are much smaller, only a limited number of injection voltage studies have been obtained. It is possible that conformations from the source are influenced by the injection process, even at our lowest injection energies. However, from these studies (and from studies of cytochrome *c* and ubiquitin) it appears that conformations from the source are observed at injection energies of ~ 300 – 600 eV and, for some stable conformers, the conformations persist at even higher energies.

Results

Formation of Ions. Typical ESI mass spectra of the disulfide-intact, disulfide-reduced solutions and the data obtained after these ions were exposed to proton-transfer reactions in the source gas cell are shown in Figure 2. ESI of the disulfide-intact solution forms the +8 to +11 charge states, while the disulfide-reduced solution yields the +10 to +18 states. These results are similar to those reported previously for lysozyme and other disulfide-bonded systems.^{21,57} After exposure to proton-transfer reagents, lower charge states are favored, demonstrating that proton-transfer reactions have occurred. For the disulfide-intact solution, we can form ions with charge states as low as +5. For the reduced solution, the charge-state distribution depends strongly on the fraction of the base that is added and we have formed ions as low as +6 in sufficient

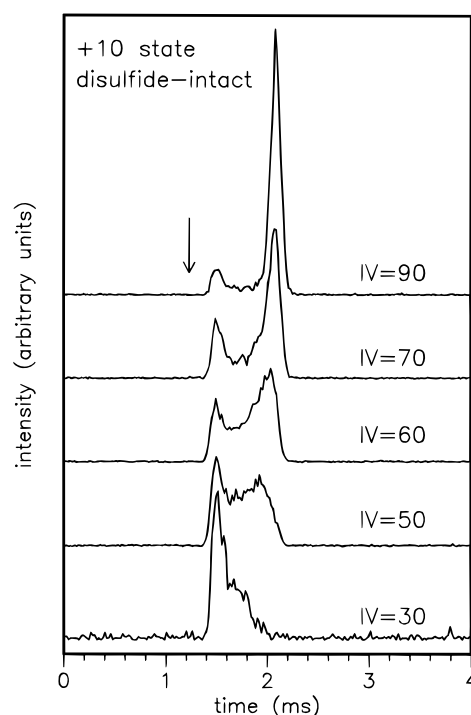


Figure 3. Drift time distributions at varying injection voltages for the +10 charge state of disulfide-intact lysozyme. The arrow shows the calculated drift time for the crystal coordinates of lysozyme (see text). These data have been scaled to a buffer gas pressure of 2.000 Torr.

abundances for these studies. Ion signals for the disulfide-reduced proton-transfer studies are much weaker than for the disulfide-intact system, and the spectrum shown in Figure 2 was collected at lower resolutions than the data for the disulfide-intact solution. We have not observed formation of the +4 state for either solution, and our mass spectrometer is currently not configured to study ions with m/z beyond ~ 4000 amu (e.g., the +3 and lower states).

Under some conditions we observe a series of peaks that correspond to the noncovalent addition of solvent molecules to the protein. The degree of clustering can be partially controlled by varying the concentration of the base in the source gas cell. The drift time distributions that are discussed below were collected under source and quadrupole resolution conditions that favor the naked protein ion. In a limited number of studies, where we have favored more adducts in the source, the drift time distributions were the same as those recorded for the naked protein.

Disulfide-Intact Ion Mobility Distributions. Figure 3 shows ion-mobility distributions as a function of injection voltage for the +10 charge state. When ions are formed from the disulfide-intact solution and injected into the drift tube at 30 V, the distributions are dominated by a peak arriving at ~ 1.5 ms. A small shoulder at longer times is also observed. As the injection voltage is increased, the peak at 1.5 ms decreases in intensity and a broad distribution that is shifted to longer times is observed. By 90 V, a new peak at ~ 2.1 ms (that was not present in the distribution at low injection voltages) is favored in the distribution. The nonzero baseline between the peaks indicates that other unresolved conformers also exist. No dissociation or proton transfer is observed at these injection voltages. Thus, the changes observed in Figure 3 must result from conformational changes. In this case at 90 V a new conformer with a smaller mobility (larger cross section) is favored.

Figure 3 also shows the drift time that is calculated from the cross section for the crystal coordinates of lysozyme as described

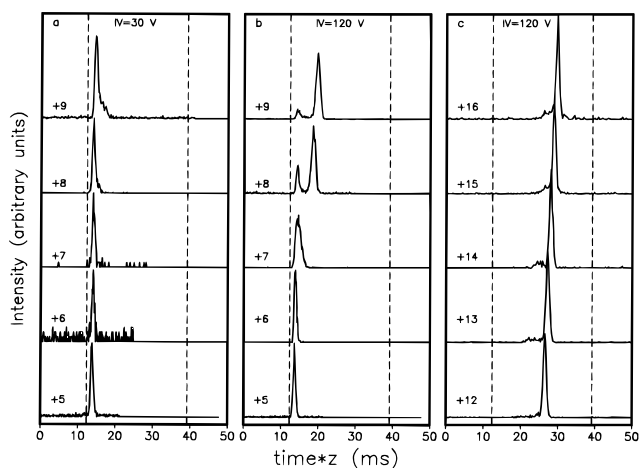


Figure 4. Charge-normalized drift time distributions for the +5 through +9 charge states of disulfide-intact lysozyme at injection voltages of 30 (part a) and 120 V (part b), and the +12 to +16 charge states of disulfide-reduced lysozyme (part c). The data have been scaled to a buffer gas pressure of 2.000 Torr. The dashed lines correspond to calculated charge-normalized drift times for the crystal coordinates of lysozyme (left) and a near-linear extended structure (right) created by stretching the protein as much as reasonably possible (see text).

above. The calculated drift time occurs at slightly shorter times than the earliest peak that we observe. Ion-mobility distributions as a function of injection voltage for the +8 and +9 charge states formed from the disulfide-intact solution exhibit behavior analogous to the data shown in Figure 3. Studies as a function of injection voltage for the +11 charge state were not carried out; however, several data sets collected at 120 V show a single peak that is similar to the peak at ~ 2.1 ms that was observed for the +10 charge state at high injection voltages.

Figure 4 (parts a and b) shows ion-mobility distributions at injection voltages of 30 and 120 V for the +8 and +9 charge states, formed directly from the disulfide-intact solution, and the +5 through +7 charge states, formed by proton-transfer reactions in the gas cell. For comparison purposes, these results are shown on a modified time scale (the drift time multiplied by the charge state) which normalizes for differences in the effective drift field (zE) for different charge states. At low injection voltages, the ion-mobility distributions for all of the disulfide-intact ions (+5 to +10 in Figures 3 and 4) are dominated by a single peak. This peak arrives near the time calculated for the crystal structure of lysozyme.

At an injection voltage of 120 V no changes in the drift time distributions for the +5 and +6 charge states are observed, suggesting that these are the most stable conformations for these charge states. For the +7 and higher charge states, ion-mobility distributions at 120 V favor conformers with mobilities lower than those observed at 30 V. The ion-mobility distribution for the +7 state at 120 V is broad, showing that a new conformer that is not fully resolved is present. Two resolved peaks can be observed for the +8 and +9 charge states, similar to the data for the +10 charge state (Figure 3).

For the disulfide-intact solution, we have also recorded ion-mobility distributions at identical injection energies (either ~ 300 or ~ 1000 eV for all charge states). These results, where energetic differences in the injection process are accounted for, show behavior analogous to the injection voltage data.

Disulfide-Reduced Ion Mobility Distributions. Figure 4 (part c) also shows ion-mobility distributions recorded (at an injection voltage of 120 V) for the +12 through +16 charge states of disulfide-reduced lysozyme. Each of the ion-mobility distributions for the disulfide-reduced ions (including the +10,

+11, +17, and +18, not shown) is dominated by a single narrow peak at longer times than for any conformers observed for the disulfide-intact ions. As the charge state increases, the peaks shift to longer times, an indication that the conformers increase in size.

Studies of disulfide-reduced ions at very low injection voltages are more difficult, due to the low ion intensities. For the +10, +14, and +16 charge states, we have recorded ion-mobility distributions at injection energies as low as 600 eV. At these low injection energies, all of the disulfide-reduced distributions are dominated by peaks corresponding to highly diffuse conformations such as those shown in Figure 4, and there is no evidence for formation of any compact conformations, such as those observed upon electrospraying the disulfide-intact solution.

From the results shown in Figure 4 it is apparent that drift times fall into three distinct conformer families. At low injection energies, all of the disulfide-intact ions (+5 to +10) favor a compact conformation that must be *highly folded*. At high injection energies, the +7 to +11 disulfide-intact ions show evidence that a structural transition has occurred. These charge states favor conformations with lower mobilities, showing that they have more open, *partially unfolded* conformations. The driving force for formation of open conformations is the increased Coulombic repulsion energy of higher charge states.^{23,27,36} The +10 to +18 charge states observed for the disulfide-reduced ions have even lower mobilities, with drift times that begin to approach the value calculated for a near-linear conformation. These ions have very open, *unfolded* conformations. The unfolded nature of the disulfide-reduced ions can be understood in terms of the large Coulombic repulsion energies for these high charge states, as well as the fact that conformations for these ions are not constrained by disulfide bonds.

Proton-Transfer Reactions of Disulfide-Reduced Ions.

Exposing the disulfide-reduced lysozyme ions to gas-phase proton-transfer reagents in the ion source favors lower charge states, from +14 to +6 depending on the conditions. Figure 5 shows a comparison of the ion-mobility distributions for the +10 to +6 charge states formed by proton transfer of the higher disulfide-reduced charge states in the gas cell (Figure 5b) to distributions recorded for the disulfide-intact ions (Figure 5a). These data were recorded under identical conditions using an injection voltage of 120 V. Also shown is the ion-mobility distribution recorded for the +14 charge state (recorded after exposure to proton-transfer reagents). All of the disulfide-reduced +10 to +14 states (recorded after exposure to the proton-transfer reagents) display peaks with drift times that are identical within experimental uncertainties to those recorded before proton-transfer reagents were added. These conformers are substantially more diffuse than the partially unfolded conformer observed for the disulfide-intact +10 state (Figure 5a).

As protons are removed, ion-mobility distributions for charge states below the +10 state show features corresponding to several types of conformations. Distributions for the +9 and +8 states display diffuse conformers at 25.2 (+9) and 23.4 ms (+8) charge states that appear to be related to the unfolded conformer observed for +10 and higher disulfide-reduced ions. These distributions also show peaks at shorter times, 21.3 (+9) and 20.4 ms (+8), which must correspond to conformations that are more compact than the unfolded family of peaks observed for the more highly charged disulfide-reduced ions. The dominant peaks for +8 and +9 (Figure 5b) correspond to

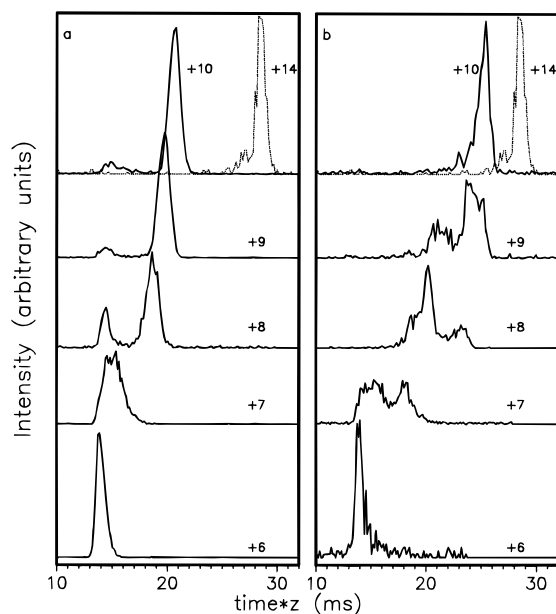


Figure 5. Charge-normalized drift time distributions for the +6 to +10 charge states of disulfide-intact (part a) and -reduced (part b) lysozyme. All data were recorded at an injection voltage of 120 V and have been scaled to a buffer gas pressure of 2.000 Torr. Ion-mobility distributions for the low charge states (+6 and +7 disulfide-intact, and +6 to +10 of the disulfide-reduced protein) were recorded after ions were exposed to proton-transfer reagents in the source gas cell.

conformers that are still more open than the partially unfolded family observed for the disulfide-intact ions. The distribution for the +8 state (Figure 5b) displays a shoulder observed at ~ 19 ms (for the disulfide-reduced ion), a drift time that is identical within experimental uncertainty to the peak observed for the partially unfolded form of disulfide-intact protein (Figure 5a).

The +7 and +6 states formed by proton-transfer reactions of the disulfide-reduced ions show additional similarities with the disulfide-intact ions. The +7 charge state shows a broad distribution with drift times that are similar to those measured for the disulfide-intact protein (~ 14 – 16.5 ms). This charge state can also form a more diffuse conformer, the peak at 18.2 ms. This more open form of the +7 ion is slightly more compact than the +8 partially folded conformer at ~ 20.4 ms (Figure 5b). The ion-mobility distribution recorded for the +6 state formed from proton-transfer reactions of the disulfide-reduced ions is superimposable with the distribution that is observed for the disulfide-intact protein.

Studies of the proton-stripped disulfide-reduced ions as a function of injection voltage show that not all of the peaks observed at 120 V are due directly to conformations formed by proton-transfer reactions in the source. Some correspond to conformations that result from exposing the lower charge state ions to the heating/cooling cycle of the injection process. Figure 6 shows data obtained for the +6 through +9 charge states at several injection voltages. In the above studies of disulfide-intact proteins, the strong ion signals allowed us to study all ions using injection voltages as low as 30 V. For the lower charge states of the disulfide-reduced ions formed by proton-transfer reactions, ion signals are much weaker and we were only able to carry out injection voltage studies to as low as 90 V. From these studies it appears that we can identify species that originate from the source, but it is possible that even at our lowest injection voltages (90 V) conformations are influenced somewhat by the injection process.

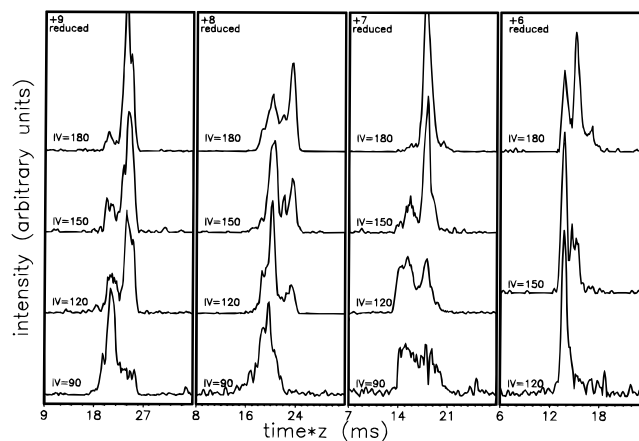


Figure 6. Charge-normalized drift time distributions as a function of injection voltage for the +6 through +10 charge states of disulfide-reduced lysozyme after it has been exposed to gas-phase proton-transfer reagents. The data have been scaled to a buffer gas pressure of 2.000 Torr.

All of the +6 through +9 charge states show that relatively compact conformations are formed at low injection voltages and, as injection voltage is increased, more unfolded forms are favored. For the +9 charge state, the most compact conformer (at ~ 20.5 ms) is still much larger than any observed for the +9 disulfide-intact ion. As the injection voltage is raised, this conformer can be converted into two new conformers that are not entirely resolved from one another at ~ 23.8 and ~ 24.5 ms. We assign the most compact of the +9 conformers (i.e., the dominant peak at ~ 21 ms in the 90 V distribution) to the conformer that results from folding in the source. The +8 charge state behaves in a similar fashion. At 90 V, a broad distribution from ~ 18 to 21 ms is favored, and as the injection voltage is increased, new peaks at 22.0 and 23.4 ms are observed. The 90 V data show no evidence for the peaks at 22.0 and 23.4 ms, but the two peaks at 20.4 and 19.0 ms (which are clearly resolved at 120 and 180 V) fall within the broad time range of the 90 V peak. Therefore, both of these conformers appear to have originated directly from the source. Similarly, we assign all three of the resolved features in the +7 distributions to conformers that may be formed from the source, since the broad distribution at 90 V includes them all. The +6 charge state favors a single compact peak at 120 V that we assign to the conformer formed in the source. At higher injection voltages other conformers can be observed.

Number of Conformers Identified for Each Charge State.

A feeling for the complexity of this system can be gained by examining drift time distributions for individual charge states of the disulfide-intact and disulfide-reduced lysozyme at several injection energies. For the disulfide-reduced +8 charge state, studies as a function of injection voltage show that four distinct conformers are present. Injection voltage studies of the disulfide-intact +8 state show that at least four unique conformers are available for this form, as well. Only the most open conformer (disulfide-intact) and most compact conformer (disulfide-reduced) have cross sections that are similar. This shows that there are at least seven unique conformations within the single +8 charge state. The +9 and +10 states show a similar complexity. For very high and low charge states, we have resolved significantly fewer states. A summary of the number of resolved conformers observed for disulfide-intact and -reduced solutions is given in Table 1.

In addition to the number of resolvable peaks in an ion-mobility distribution, the peak widths give information about how many conformers are present within each peak of the drift

TABLE 1: Number of Resolved Conformers for Disulfide-Intact and -Reduced Lysozyme Ions

charge state	disulfide intact	disulfide reduced	total of unique ^a
+5	1	—	1
+6	1	3	3
+7	2	3	3
+8	4	4	7
+9	4	3	7
+10	4	1	5
+11	1	1	2
+12 and higher	—	1	1

^a This refers to the total number of conformations having different cross sections.

time distribution. The calculated distribution for transport of a single conformer through the drift tube can be expressed by eq 4,⁵¹

$$\Phi(t) = \int dt_p P(t_p) \frac{C}{(Dt)^{1/2}} (v_D + L/t) \left[1 - \exp\left(\frac{-r_0^2}{4Dt}\right) \right] \times \exp\left(\frac{-(L - v_D t)^2}{4Dt}\right) \quad (4)$$

In this equation, $\Phi(t)$ is the flux of ions passing through the exit aperture as a function of time, r_0 is the radius of the entrance aperture, v_D is the measured drift velocity, C is a constant, $P(t_p) dt_p$ is the distribution function for the pulse of ions entering the drift tube, and D is the diffusion constant, which under low-field conditions is related to the measured mobility by the expression $D = Kk_B T/ze$, where K is the mobility, k_B is Boltzmann's constant, and ze is the charge. When the measured drift time distribution is significantly broader than the calculated distribution, it indicates that at least two conformers with similar collision cross sections (or conformers that are interconverting over the time scale of the experiment) are present. When the drift time distribution calculated using this expression is in good agreement with the measured distribution, it suggests that only a single conformer is present. However, two conformers having identical collision cross sections cannot be ruled out.

When calculated distributions are compared with experimental peaks, several trends are apparent. Peaks for the most compact conformers observed for the +5 through +10 charge states (disulfide-intact) have full widths at half-maxima (fwhm) that are a factor of ~ 2.8 larger than the calculated values. The fwhm of peaks associated with disulfide-intact partially unfolded conformer types (+8 through +11) are a factor of ~ 3.8 times larger than the calculated values. These results indicate that multiple conformations (or related structures that interconvert on the time scale of the experiment) must be present. The peaks associated with the very diffuse structures observed when disulfide-reduced ions are injected at 120 V are represented much more accurately than those for the disulfide-intact protein. The fwhm of peaks in the disulfide-reduced drift time distributions are factors of ~ 1.6 times larger than the calculated values, suggesting that only closely related conformers are present.

Discussion

Collision Cross Sections. Figure 7 shows the collision cross sections for the +5 through +18 charge states that are derived using eq 3. The cross sections shown correspond to the peak centers for features that were clearly resolved at injection voltages of 30 or 120 V. Cross sections associated with species in the broad, unresolved features observed at other injection voltages for the +7 to +10 states of the disulfide-intact ions

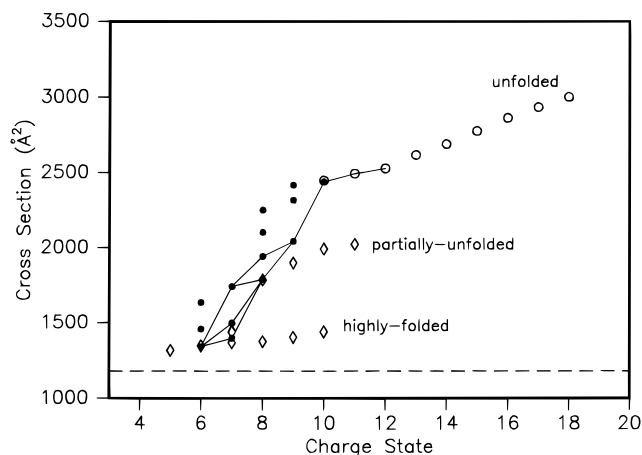


Figure 7. Summary of cross sections determined for all ions observed in these studies. The open diamonds correspond to disulfide-intact lysozyme ions and correspond to highly folded and partially unfolded conformations (see text). The open circles correspond to unfolded conformers that were formed by electrospraying a disulfide-reduced solution of lysozyme. The solid circles correspond to peaks observed after the disulfide-reduced peaks (open circles) are exposed to gas-phase charge-stripping reagents in the source gas cell. The solid line corresponds to those species that appear to be formed directly from proton-transfer reactions in the source (see text). The dashed line is the calculated cross section for the crystal coordinates of lysozyme.

are not plotted. As discussed above, three distinct conformer types are observed: a highly folded compact conformer (observed for the +5 through +10 charge states) with cross sections that are near the value calculated for the crystal coordinates, an intermediately sized partially unfolded conformer (observed for the +8 through +11 charge states) formed by injecting compact conformers into the drift tube at high injection voltages, and a highly diffuse unfolded conformer (observed for the +10 through +18 charge states) that is only formed for the disulfide-reduced solution.

Figure 7 also shows cross sections for the disulfide-reduced ions after they have been exposed to proton-transfer reactions in the source gas cell. The +9 and +8 charge states display a diffuse conformer that correlates with the unfolded conformations measured for higher disulfide-reduced ions. Several other conformers with smaller cross sections are also observed, including a +8 conformer that is near the cross section measured for the partially unfolded conformer observed for the disulfide-intact +8 state. The +7 and +6 charge states can exist in a conformation that appears to correlate with the partially unfolded conformers observed for the disulfide-intact ions at 120 V. Both of these ions also have conformations with cross sections that are identical within experimental uncertainty to the cross sections for the most compact conformers of the +7 and +6 disulfide-intact ions. The solid lines connecting some of the points correspond to those features that are observed at the lowest injection voltages possible for these studies (Figure 6) and are discussed in more detail below.

Do Gas-Phase Conformations Resemble Conformations in Solution? Factors such as the solution pH,⁵⁸ solvent composition,⁵⁹ and temperature^{60,61,62} have been shown to influence the distribution of charges that are produced by ESI. However, the degree to which conformations of the gas-phase protein ions resemble the protein's conformation in the ESI solution is less obvious.⁶³ Ion energy loss,³⁶ ion mobility,^{23,27} and high-energy surface impact studies⁴⁰ of cytochrome *c* have shown that high charge states formed by ESI of acidic solutions favor conformations that are more diffuse than the native solution conformer, even though acid denaturation of cytochrome *c* forms the more compact A state.^{64,65} When cyto-

chrome *c* is electrosprayed from a native solution, lower charge states, with collision cross sections that are similar to values that are calculated for the native solution conformer, are observed, suggesting that the compact nature of the solution conformation may be preserved. Similar results have been obtained for myoglobin from microscopy studies of high-energy surface impacts⁴⁰ and ion-mobility studies.⁶⁶

The lysozyme system provides an extreme test of the resiliency of the solution conformation in the gas phase, since the reduced and oxidized form of the protein differ by four covalent disulfide bonds that stabilize and restrict the conformation of the oxidized form in solution. Previous fragmentation studies of disulfide-bonded and -reduced proteins have shown different fragmentation patterns for these ions.¹⁹ Microscopy studies of ion impacts of lysozyme formed from native solutions are consistent with a compact conformer.⁴⁰ Proton-transfer studies of the disulfide-intact and -reduced molecules have shown differences in the ion reactivities,^{45,46} and the model of the protein that emerges from gas-phase basicity measurements of the disulfide-intact ions is most consistent with a compact structure, while basicities of the reduced protein ions are more consistent with a linear model.²¹

The cross sections that we have measured for the disulfide-intact protein show that it favors highly folded compact conformations (for the +5 through +10 charge states). The +8 through +10 charge states of the disulfide-intact protein undergo a structural transition when injected into the drift tube at high injection energies, forming a more open conformer. However, even this form of the protein is only partially unfolded. Cross sections for the disulfide-reduced protein (+10 through +18) are much larger than any observed for the disulfide-intact protein (Figure 7). These results show that disulfide bonds, which are retained from the solution phase, are an important constraint for the conformation of the gas-phase ions.

Comparison of Ion-Mobility Cross Sections with Gas-Phase Basicity Models. A closer comparison of our results to the gas-phase basicity measurements²¹ shows additional similarities and differences. The cross sections that we have measured for the disulfide-reduced protein show that it is highly extended, but still significantly more compact than the calculated cross section for the limiting near-linear conformer. The physical size of the unfolded conformer depends strongly on the charge state, a result that is also found for other proteins and which is explained by increasing Coulombic repulsion which causes the unfolded form to expand. In a qualitative sense, we agree with the gas-phase basicity model in that a more open form of the disulfide-reduced ions is favored. However, the cross sections that we measure are far below the value calculated for a one-dimensional string, showing that although these ions are largely unfolded, they still retain some secondary and tertiary structure.

The gas-phase basicity model also predicts that removing protons from the disulfide-intact protein causes the protein to denature, presumably forming a more open form. Our results show the opposite behavior: the protein favors a more compact conformer with a cross section that approaches the calculated value for the crystal coordinates.

An additional comparison can be made between the total numbers of conformers observed within each charge using these different techniques. The basicity studies report a single reactive conformation for the +15 through +13 and the +10 charge states (disulfide-reduced), in agreement with our observation of a single peak in the drift time distributions for these states (Table 1). However, for the +11 and +12 states, basicity measurements appear to be sensitive to several conformations,

where only one is resolved in the mobility experiment. For the +10 through +6 states formed from both the disulfide-intact and -reduced solutions, both techniques find more conformers, but for these states it appears that more conformers are resolved based on differences in their cross sections rather than their different basicities. Both techniques show evidence of overlapping conformers between the disulfide-reduced and disulfide-intact protein for the +8, +7, and +6 charge states. Both methods also show that, for higher charge states, no overlapping features are measured for the disulfide-intact and disulfide-reduced protein.

Proton-Transfer and Gas-Phase Folding. A remarkable and unexpected⁶⁷ result of proton-transfer studies^{20–22} is that highly charged elongated conformations appear to fold as protons are removed. As discussed previously,²¹ it becomes thermodynamically possible for gas-phase protein ions to fold when attractive forces, such as van der Waals and hydrogen-bonding interactions, become greater than unfavorable entropy and Coulombic repulsion interactions. Additionally, our experiments are limited kinetically by the short time scales involved in beam experiments. After their initial formation, we estimate that ions spend only ~10–30 ms in the proton-exchange region before being injected into the drift tube.⁶⁸ Folding must occur rapidly upon proton transfer in order to be observed here.

One of the most intriguing features of our data is that as the disulfide-reduced ions refold in the gas phase, the compact conformations that are observed have cross sections that are identical to those measured for the disulfide-intact ions. Because ion-mobility measurements are sensitive to average shapes, it is expected that some conformations which are folded differently could have identical collision cross sections. However, we cannot resist noting the striking similarities observed for ion-mobility distributions for the +6 and +7 charge states for the disulfide-intact and -reduced ions. These peaks in the ion-mobility distributions for the disulfide-reduced and -intact ions are essentially identical in position and shape. It is possible that when protons are removed from the disulfide-reduced ions the protein folds up to a conformation that is similar to that observed for the disulfide-bonded ions.

Although it seems unlikely, it is possible that disulfide bonds reform during proton-transfer reactions. FTICR measurements of the *m/z* increase observed upon electrospraying a disulfide-reduced lysozyme solution compared with conditions that favor the native protein show an 8 amu increase in mass for the former conditions, demonstrating that all four disulfide bonds have been reduced.²¹ Further corroboration of the reduced nature of the protein comes from comparing data that is recorded as a function of injection voltage for reduced and oxidized solutions. At high injection voltages, the +6, +7, and +8 states formed after proton-transfer reactions of ions formed from the disulfide-reduced solution show open conformations that are not observed under identical conditions for the disulfide-intact solution. Thus, there is no experimental evidence supporting the idea that disulfide bonds reform during the proton-transfer process.

Proposed Folding and Unfolding Pathways in the Gas Phase. Studies as a function of injection voltage for the disulfide-reduced protein (Figure 6) provide some information about the origin of the features observed in the drift time distributions. In general, a higher degree of folding is observed at low injection voltages than at high voltages. This shows that some of the features that are observed probably do not result directly from charge-stripping induced folding processes, but rather are generated by unfolding induced by the rapid heating/cooling cycle of the injection process. The lines connecting some of the structures in Figure 7 correspond to those species

that appear to be formed directly by charge-stripping reactions in the source gas cell, as discussed above.

Typically, the rapid heating/cooling cycle upon injection of the ions into the drift tube is thought of as an annealing process, and high injection voltages favor the most stable isomers. However, the charge-stripping-induced folding results reported here suggest that in this system this is not the case. Diffuse conformations should not spontaneously fold up to compact conformers that are thermodynamically unfavorable. The results suggest that the unfolded (+8 and +9) species (formed at high injection voltages) correspond to metastable states that are trapped during the heating/cooling cycle of the injection process. For such a large molecule like lysozyme, kinetic trapping in the gas phase is not surprising. Recently temperature-dependent studies of cytochrome *c* have shown that the injection process can lead to formation of metastable conformations for some charge states.⁶⁹ Partial unfolding or misfolding could easily occur as the protein is heated during the injection process, and the lowest energy state may not re-form before further collisions quench the protein as a metastable state. When completely denatured lysozyme is refolded in solution, the observed kinetic heterogeneity shows that kinetically trapped states are present, and several origins, including misformation of disulfide bonds which result in knotting of the protein, have been proposed.^{15–18}

The +6 through +9 species formed by charge stripping the disulfide-reduced ions in the source must correspond either to conformers that are unreactive with respect to further charge exchange or to species that exit the source before undergoing sufficient collisions with the base to exchange to completion. The gas-phase basicity measurements for lysozyme have shown that some conformers within a given charge state react more rapidly than others.²¹ However, because the mass spectra we observe are sensitive to variations in the concentrations of the bases, we believe the latter explanation is most consistent with our data. If true, then the lines shown in Figure 7 for species that are generated directly from the electrospray source correspond to the gas-phase folding pathways induced by sequentially removing protons. The unfolded conformers that are observed are formed by collisional heating during the injection process.

The folding pathway can be summarized as follows. Removing a single charge from the diffuse (2445 Å²) +10 charge state results in a +9 conformation with a 2043 Å² cross section that is ~16% smaller. As another charge is removed, the +8 charge state favors two structures having cross sections of 1943 and 1789 Å² that are 4% and 12% more compact than the +9 charge state. The +7 charge state shows a broad distribution. The most compact of these conformations (with a cross section of 1397 Å²) correspond to the compact conformer observed for the disulfide-intact protein and shows that the protein has collapsed by at least 22% upon removal of a single charge. The most diffuse (+7) conformer is similar to the partially unfolded conformations observed at high injection voltages for the +8 through +11 charge states of the disulfide-intact protein. Removal of another charge from the most compact +7 charge state causes the protein to contract slightly (~4%) and forms the highly folded +6 charge state. The other larger +7 states can also form the +6 charge state but must collapse significantly more (up to ~23%). Our data suggests that gas-phase folding involves several pathways, as observed in solution.¹⁷

A simple scheme that shows these folding and unfolding events is shown in Figure 8. In Figure 8, the number of protons increases from $n - 2$ to n , from left to right, and folding and unfolding transitions are shown vertically. Thus protons are removed from right to left, comparable to the cross section data

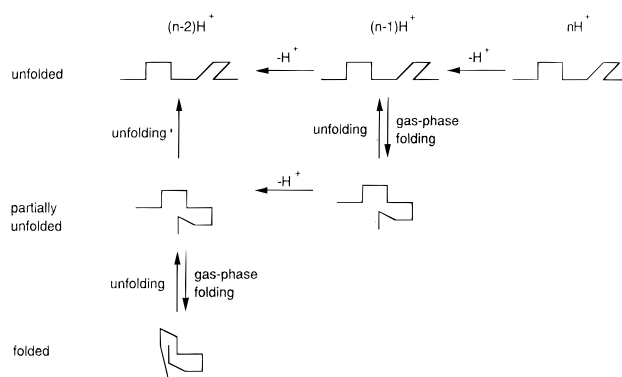


Figure 8. Schematic representation of the folding and collisional unfolding observed in these studies as a result of proton-transfer reactions.

shown in Figure 7. As a proton is removed from an unfolded, $(n)H^+$ state during a proton-transfer reaction, the balance between the repulsive–Coulombic and attractive–folding interactions is disrupted, causing the $(n - 1)H^+$ state to spontaneously fold up to a more compact conformation. The scheme in Figure 8 shows this as a two-step process that assumes that proton transfer is more rapid than folding. As the resulting compact conformers enter the drift tube and are exposed to the heating/cooling cycle of the injection process, some may open up, giving rise to the unfolded $(n - 1)H^+$ conformers. This explains the unfolded conformers observed for the +8 and +9 charge states. The $(n - 1)H^+$ unfolded forms (such as for the +8 and +9 states) are probably metastable kinetically trapped forms that are partially unfolded or misfolded, and if given enough time, they may refold. When a proton is removed from the $(n - 1)H^+$ state, a similar transformation can occur, leading to an even more compact $(n - 2)H^+$ state. In this way, the charge state becomes the reaction coordinate from an unfolded, to a partially unfolded, to a highly folded protein, and some of the conformations observed for each charge states are intermediates that are energetically trapped because of differences in Coulombic repulsion.

Conclusions

Ion mobility studies of disulfide-intact and disulfide-reduced lysozyme ions show that conformations that are observed in the gas phase are highly dependent on the presence of disulfide bonds. The +5 through +10 charge states of the disulfide-intact protein show a highly folded conformer with a cross section that is near the value calculated for the crystal coordinates of lysozyme. An additional partially unfolded conformer is favored for the +8 through +11 charge states at high injection voltages. The +10 through +18 charge states of the disulfide-reduced protein favor highly diffuse, unfolded forms of the protein, as is expected since there are no disulfide bonds to impose structural restrictions. When the disulfide-reduced protein is exposed to proton-transfer reagents in the source, the lower charge states that are observed have dramatically smaller cross sections, showing that they can fold in the gas phase. A remarkable feature of the folding process is that some of the conformations that result from folding of the disulfide-reduced protein have cross sections that appear to correlate with the partially unfolded form of the disulfide-intact protein. When effects of the injection process are taken into account, it is possible to examine which species are due to folding and which are due to species that are kinetically trapped as partially unfolded or misfolded conformers. From these results we propose specific gas-phase folding pathways that

involve a series of intermediates differing in charge state and conformation.

One of the differences in the chemistry that is observed in the gas phase and that observed in solution is that chemical intermediates are routinely trapped and characterized in solution, while chemical intermediates in the gas phase are typically elusive and difficult to study because of their short lifetimes. Characterizing intermediates in protein folding in solution presents a unique challenge because of the overwhelming sizes and dynamic natures of these species. Studies of conformation in the gas phase may offer advantages in understanding the folding process since it appears that as charges are stripped, from a very diffuse, highly charged unfolded conformation, to form a compact, highly folded low-charge conformation, intermediates can be trapped as different charge states. These intermediates appear to be stable because of a well-defined interplay between Coulombic—repulsion and attractive interactions in the homogeneous vacuum environment. The relationship of intermediates and folding pathways observed in the gas phase to those that are important in solution is unknown.

Acknowledgment. We gratefully acknowledge the National Science Foundation (Grant No. CHE-9625199) for support of this work.

References and Notes

- Fenn, J. B.; Mann, M.; Meng, C. K.; Wong, S. F.; Whitehouse, C. M. *Science* **1989**, *246*, 64.
- Karas, M.; Hillenkamp, F. *Anal. Chem.* **1988**, *60*, 2299.
- Chait, B. T.; Kent, S. B. H. *Science* **1992**, *257*, 1885.
- Biemann, K. *Annu. Rev. Biochem.* **1992**, *61*, 997.
- Siuzdak, G. *Proc. Natl. Acad. Sci. U.S.A.* **1994**, *91*, 11290.
- Biemann, K.; Scobel, H. A. *Science* **1987**, *237*, 992.
- Brulingame, A. L.; Boyd, R. K.; Gaskell, S. J. *Anal. Chem.* **1994**, *66*, 634R.
- McLuckey, S. A.; Van Berkel, G. J.; Glish, G. L. *J. Am. Chem. Soc. Mass Spectrom.* **1992**, *3*, 60.
- McLuckey, S. A.; Habibgoudarzi, S. *J. Am. Chem. Soc.* **1993**, *115*, 12085.
- Senko, M. W.; Beu, S. C.; McLafferty, F. W. *Anal. Chem.* **1994**, *66*, 415.
- Hagen, D. F. *Anal. Chem.* **1979**, *51*, 870.
- St. Louis, R. H.; Hill, H. H. *Crit. Rev. Anal. Chem.* **1990**, *21*, 321.
- von Helden, G.; Hsu, M. T.; Kemper, P. R.; Bowers, M. T. *J. Chem. Phys.* **1991**, *95*, 3835.
- Jarrold, M. F.; Constant, V. A. *Phys. Rev. Lett.* **1992**, *67*, 2994.
- Kieffhaber, T. *Proc. Natl. Acad. Sci. U.S.A.* **1995**, *92*, 9029.
- Itzhaki, L. S.; Evans, P. A.; Dobson, C. M.; Radford, S. E. *Biochemistry* **1994**, *33*, 5212.
- Radford, S. E.; Dobson, C. M.; Evans, P. A. *Nature* **1992**, *358*, 302.
- Chaffotte, A. F.; Guillou, Y.; Goldberg, M. E. *Biochemistry* **1992**, *31*, 9694.
- Loo, J. A.; Edmonds, C. G.; Smith, R. D. *Science* **1990**, *248*, 201.
- Wood, T. D.; Chorush, R. A.; Wampler, F. M. III; Little, D. P.; O'Connor, P. B.; McLafferty, F. W. *Proc. Natl. Acad. Sci. U.S.A.* **1995**, *92*, 2451.
- Gross, D. S.; Schnier, P. D.; Rodriguez-Cruz, S. E.; Fagerquist, C. K.; Williams, E. R. *Proc. Natl. Acad. Sci. U.S.A.* **1996**, *93*, 3143.
- Shelimov, K. B.; Jarrold, M. F. *J. Am. Chem. Soc.* **1996**, *118*, 10313.
- Clemmer, D. E.; Hudgins, R. R.; Jarrold, M. F. *J. Am. Chem. Soc.* **1995**, *117*, 10141.
- In addition to refs 13 and 14, see for example: von Helden, G.; Hsu, M.-T.; Gotts, N.; Bowers, M. T. *J. Phys. Chem.* **1993**, *97*, 8182. Lee, S. H.; Gotts, N. G.; von Helden, G.; Bowers, M. T. *Science* **1995**, *267*, 999. Jarrold, M. F. *J. Phys. Chem.* **1995**, *99*, 11. Clemmer, D. E.; Jarrold, M. F. *J. Am. Chem. Soc.* **1995**, *117*, 8841 and references therein.
- von Helden, G.; Wyttenbach, T.; Bowers, M. T. *Science* **1995**, *267*, 1483.
- Lee, S.; Wyttenbach, T.; von Helden, G.; Bowers, M. T. *J. Am. Chem. Soc.* **1995**, *117*, 10159.
- Shelimov, K. B.; Clemmer, D. E.; Hudgins, R. R.; Jarrold, M. F. *J. Am. Chem. Soc.* **1997**, *119*, 2240.
- Valentine, S. J.; Clemmer, D. E. *J. Am. Chem. Soc.*, in press.
- Jarrold, M. F.; Honea, E. C. *J. Phys. Chem.* **1991**, *95*, 9181.
- Jarrold, M. F.; Constant, V. A. *Phys. Rev. Lett.* **1991**, *67*, 2994.
- Schnier, P. F.; Gross, D. S.; Williams, E. R. *J. Am. Chem. Soc.* **1995**, *117*, 6747.
- See for example: Campbell, S.; Rodgers, M. T.; Marzluff, E. M.; Beauchamp, J. L. *J. Am. Chem. Soc.* **1995**, *117*, 12840. Gur, E. H.; de Koning, L. J.; Nibbering, N. M. M. *J. Am. Soc. Mass Spectrom.* **1995**, *6*, 466. Gard, E.; Green, M. K.; Bregar, J.; Lebrilla, C. B. *J. Am. Soc. Mass Spectrom.* **1994**, *5*, 623.
- Winger, B. E.; Light-Wahl, J. J.; Rockwood, A. L.; Smith, R. D. *J. Am. Chem. Soc.* **1992**, *114*, 5897.
- Suckau, D.; Shi, Y.; Beu, S. C.; Senko, M. W.; Quinn, J. P.; Wampler, F. M. III; McLafferty, F. W. *Proc. Natl. Acad. Sci. U.S.A.* **1993**, *90*, 790.
- Cassady, C. J.; Carr, S. R. *J. Mass Spectrom.* **1996**, *31*, 247.
- Covey, T. R.; Douglas, D. J. *J. Am. Soc. Mass Spectrom.* **1993**, *4*, 616.
- Douglas, D. J. *J. Am. Soc. Mass Spectrom.* **1994**, *5*, 17.
- Collings, B. A.; Douglas, D. J. *J. Am. Chem. Soc.* **1996**, *118*, 4488.
- Cox, K. A.; Julian, R. K.; Cooks, R. G.; Kaiser, R. E. *J. Am. Soc. Mass Spectrom.* **1994**, *5*, 127.
- Sullivan, P. A.; Axelsson, J.; Altmann, S.; Quist, A. P.; Sunqvist, B. U. R.; Reimann, C. T. *J. Am. Chem. Soc. Mass Spectrom.* **1996**, *7*, 329.
- Kaufman, S. L.; Skogen, J. W.; Dorman, F. D.; Zarrin, F.; Lewis, K. C. *Anal. Chem.* **1996**, *68*, 1895.
- Smith, R. D.; Loo, R. R.; Busman, M.; Udseth, H. R. *Mass Spectrom. Rev.* **1991**, *10*, 359.
- Smith, R. D.; Loo, J. A.; Loo, R. R.; Udseth, H. R. *Mass Spectrom. Rev.* **1992**, *11*, 434.
- Wittmer, D.; Chen, Y. H.; Luckenbill, B. K.; Hill, H. H. *Anal. Chem.* **1994**, *66*, 2348.
- Ogorzalek Loo, R. R.; Winger, B. E.; Smith, R. D. *J. Am. Soc. Mass Spectrom.* **1994**, *5*, 207.
- Ogorzalek Loo, R. R.; Winger, B. E.; Smith, R. D. *J. Am. Soc. Mass Spectrom.* **1994**, *5*, 1064.
- Zhang, X.; Cassady, C. J. *J. Am. Soc. Mass Spectrom.* **1996**, *7*, 1211.
- Smith, R. D.; Loo, J. A.; Edmonds, C. G.; Barinaga, C. J.; Udseth, H. R. *Anal. Chem.* **1990**, *62*, 882–889.
- Lias, S. B.; Liebman, J. F.; Levin, R. D. *J. Phys. Chem. Ref. Data* **1984**, *13*, 695.
- Decouzon, M.; Bal, J. F.; Maria, P. C.; Raczynska, E. D. *Rapid Commun. Mass Spectrom.* **1993**, *7*, 599.
- Mason, E. A.; McDaniel, E. W. *Transport Properties of Ions in Gases*; Wiley: New York, 1988.
- Loo, J. A.; Edmonds, C. G.; Udseth, H. R.; Smith, R. D. *Anal. Chem.* **1990**, *62*, 693.
- The crystal coordinates for turkey lysozyme are taken from the world wide web: <http://expasy.hcuge.ch/cgi-bin/get-pdb-entry?1lz3>.
- The near-linear protein was created using Insight II, BIOSYM/MSI, San Diego, CA (1995).
- These values are derived from the van der Waals radii used by Insight II for calculating structures of biological molecules.
- Valentine, S. J.; Clemmer, D. E. Accepted by *J. Am. Soc. Mass Spectrom.*
- Loo, R. R. O.; Smith, R. D. *J. Am. Soc. Mass Spectrom.* **1994**, *5*, 207. Loo, R. R. O.; Winger, B. E.; Smith, R. D. *J. Am. Soc. Mass Spectrom.* **1994**, *5*, 1064.
- Chowdhury, S. K.; Katta, V.; Chait, B. T. *J. Am. Chem. Soc.* **1990**, *112*, 9012.
- Loo, J. A.; Loo, R. R. O.; Udseth, H. R.; Edmonds, C. G.; Smith, R. D. *Rapid Commun. Mass Spectrom.* **1991**, *5*, 101.
- Miraz, U. A.; Cohen, S. L.; Chait, B. T. *Anal. Chem.* **1993**, *65*, 1.
- LeBlanc, J. C. Y.; Beuchemin, D.; Siu, K. W. M.; Guevremont, R.; Berman, S. S. *Org. Mass Spectrom.* **1991**, *5*, 582.
- Rockwood, A. S.; Busman, M.; Udseth, H. R.; Smith, R. D. *Rapid Commun. Mass Spectrom.* **1991**, *5*, 582.
- Wolynes, P. G. *Proc. Natl. Acad. Sci. U.S.A.* **1995**, *92*, 2426.
- Myer, Y. P.; Saturno, A. F. *J. Protein Chem.* **1990**, *9*, 379.
- Drew, H. R.; Dickerson, R. E. *J. Biol. Chem.* **1978**, *253*, 8420. Tsong, T. Y. *Biochemistry* **1973**, *12*, 2209. Dwyer, H. J.; Beattie, J. K. *J. Biol. Chem.* **1982**, *257*, 2267.
- Shelimov, K. B.; Jarrold, M. F. Submitted for publication.
- Smith, R. D.; Light-Wahl, K. J. *Biol. Mass Spectrom.* **1993**, *22*, 493.
- This estimate is made by assuming that ions enter the gas cell at thermal energies and are pulled across the cell by a small potential drop between the entrance and exit plates of the gas cell. Changes in the charge state have not been considered, and other implicit assumptions are that the mobilities of the ions through the gas mixture in the gas cell are similar to those measured in He.
- Shelimov, K. B.; Jarrold, M. F. Private communication.